Journal Pre-proofs

Direct regeneration and flash upcycling of mixed spent graphite with a uniform energy-storage property

Zhen Shang, Zhang Naizhe, Zhiwen Ying, Daijiang Zou, Feng Dai, Jihong Xie, Jie Shao, Xuegang Liu, Shengming Xu

PII: S1385-8947(24)10623-7
DOI: https://doi.org/10.1016/j.cej.2024.159132
Reference: CEJ 159132

To appear in: *Chemical Engineering Journal*

Received Date: 16 October 2024
Revised Date: 10 December 2024
Accepted Date: 29 December 2024

Please cite this article as: Z. Shang, Z. Naizhe, Z. Ying, D. Zou, F. Dai, J. Xie, J. Shao, X. Liu, S. Xu, Direct regeneration and flash upcycling of mixed spent graphite with a uniform energy-storage property, *Chemical Engineering Journal* (2024), doi: https://doi.org/10.1016/j.cej.2024.159132

Direct regeneration and flash upcycling of mixed spent graphite with a uniform energy-storage property

Zhen Shang[a], Zhang Naizhe[a], Zhiwen Ying[a], Daijiang Zou[b], Feng Dai [b], Jihong Xie[c], Jie Shao[c*], Xuegang Liu[a*], and Shengming Xu[a*]

[a] Institute of Nuclear and New Energy Technology, Tsinghua University, Beijing, 100084, China

[b] Sichuan New Energy Vehicle Innovation Center Co., Ltd., Yibin, 644000, China

[c] SAIC GM Wuling Automobile CO., Ltd, Liuzhou, 545007, China

Email: smxu@ mail tsinghua.edu.cn; jie.shao@sgmw.com.cn; liuxg@mail.tsinghua.edu.cn

Abstract: Direct regeneration of spent graphite is a crucial strategy for utilizing spent lithium-ion batteries, conserving natural resources and reducing waste, providing significant economic and environmental benefits. The main challenges in this process include low adaptability methods to recycle different types of spent graphite and high energy consumption. In this study, we successfully converted scrap graphite, disassembled anode graphite, and graphite from hydrometallurgical slag into graphite uniform properties using flash Joule heating. This flash upcycling process allows for rapid regeneration only within seconds. The regenerated graphite demonstrated excellent performance, exhibiting 358 mAh/g specific capacity at 0.1C and 94.83% capacity retention after 100 cycles. Economic and environmental assessments of the three methods showed this flash recycling significantly increases profitability to $7.75/kg and reduces greenhouse gas emissions and total energy consumption. The underlying mechanism involves flash Joule heating, which generates a large current in graphite for defect healing and crystalline structure restoration and removes coating impurities through rapid annealing. This technique efficiently regenerates various types of spent anode graphite with low energy consumption, providing valuable insights into large-scale spent graphite recycling.

Keywords: spent lithium-ion batteries, various spent graphite, flash joule heating, upcycling, uniformity property

Graphical Abstract

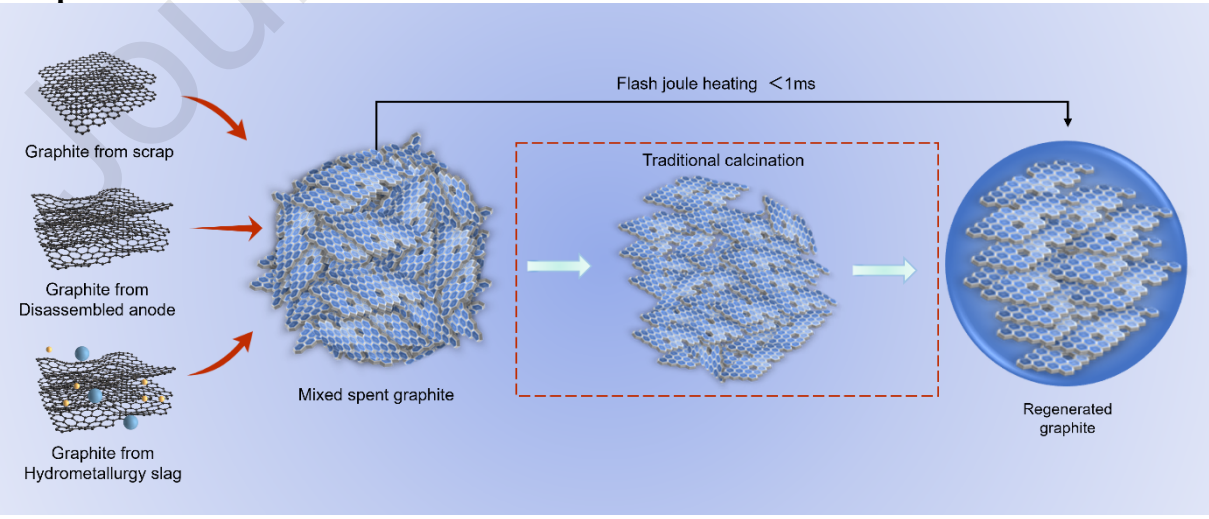

29

30

31

32

33

1. Introduction

The accelerating growth of electric vehicles and energy storage facilities, propelled by the increasing emphasis on achieving carbon neutrality, has led to a rise in significant need of lithium-ion batteries (LIBs). [1] However, service life of lithium-ion batteries (LIBs), which ranges from 5 to 10 years depending on usage, presents a complex challenge. It is projected that by 2024, spent LIBs will reach 1.08 million tons, posing a significant environmental threat.[2] Conversely, spent batteries, often referred to as " urban mines", contain valuable elements such as manganese (Mn), cobalt (Co), nickel (Ni), and lithium (Li) in the cathodes, as well as graphite in the anodes, offering substantial recycling opportunities. [3] Reclaiming these materials holds immense significance, transforming waste into valuable resources, and offering both economic and environmental advantages. Existing traditional recycling methods, such as pyrometallurgy and hydrometallurgy, involve high-temperature roasting or acid/alkaline leaching. The primary focus concentrates on valuable precious metals in the cathodes, whereas the anodes, typically made of graphite, are often overlooked in spent LIBs. [4, 5]

In pyrometallurgy, graphite is employed as an in situ reducing agent to lower the valence of transition metals, thereby ensuring that metal elements in lower valence states remain stable in solution. However, the spent graphite is often left in the slag with high-content impurities after traditional hydrometallurgy methods. Even several research groups have been working on the design of recycling graphite, the spent graphite could produce other functional materials, including graphite based adsorbents/ capacitors/ graphene/polymer composite materials, [6] the increasing demand for regenerated graphite for LIB production exceeds the demand for these materials. Despite morphological and slight structural changes, spent graphite particles retain their bulk graphite structure, a spherical shape offering advantages for direct reuse as battery-grade material compared to raw graphite materials.[7] Given the substantial demand for graphite in LIBs and the significant quantity of spent graphite, repurposing spent graphite into battery-grade material could increase the supply of battery anode graphite and reduce potential hazards from solid waste.

Regenerating spent graphite faces a considerable obstacle due to variations among different spent graphite sources, production processes, and separation methods, leading to difficulties in a unified regeneration process.[8] The failure mechanisms of graphite anode materials encompass several issues: degeneration of solid electrolyte interphase (SEI), formation of lithium metal dendrites, co-intercalation of solvents, exfoliation of graphite, and cracking of particles. [9, 10] The impurities, excessive SEI formation, and structural degradation in spent graphite anodes diminish battery performance. To repurpose spent graphite into battery-grade material, an effective recycling method must address impurity removal and structural/surface film restoration. Acid leaching treatments effectively eliminate impurities but are limited in their ability to recover the crystalline structure of graphite. [11] Traditional structural reconstruction demands high energy (~3000 K, lasting several days) to meet anode graphite requirements.[12] Although surface film reconditioning (metal-based or carbon-based coating) enhances conductivity, it still encounters issues with disordered graphite. Existing traditional methods, high-temperature sintering, acid leaching, and surface film reconditioning are hindered by their lengthy processing times, precise control needs, high costs, and difficulties in handling diverse spent graphite, posing a substantial gap in large-scale production. Therefore, developing a rapid, cost-effective, adaptable process for recycling various spent graphite from LIBs is imperative.

Herein, we present a novel, super-fast modified flash joule heating (FJH) technique to treat various anode graphite wastes from spent LIBs, converting them into battery-grade graphite

with uniform properties within seconds (Fig 1). By leveraging extreme temperatures for short durations, this technique decomposes the solid electrolyte interphase (SEI), binder, and intercalated molecules, and restores the layered structure of graphite, preserving the new morphology of the graphite particles. We meticulously explored disparities between spent and recovered graphite in terms of structure, surface properties, and electrochemical performance to substantiate our findings. With good performance of regenerated graphite, this work might make a step to fulfill the gap in recycling spent graphite anodes for large-scale battery-grade material production.

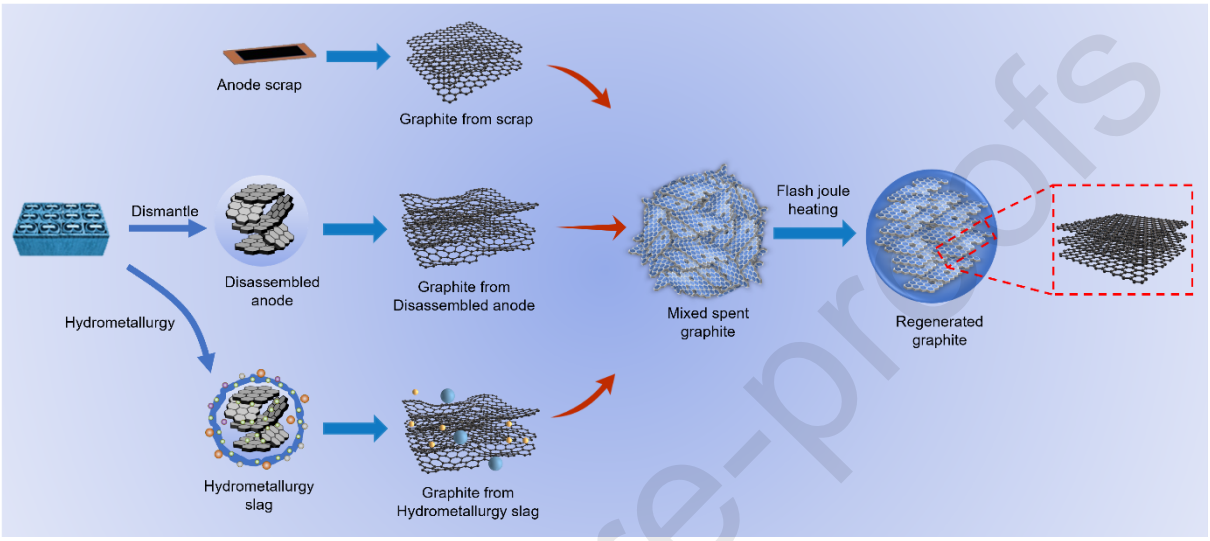

Fig. 1. Schematic of flash upcycling of various spent graphite into a uniform energy-storage property via flash heating

2. Experimental Section

2.1. Materials

Different spent anode materials were obtained from Shenzhen Xinmao Co., Ltd. (graphite scrap), CALB Group Co., Ltd. (graphite from disassembled anodes), and Huayou Cobalt Co., Ltd. (graphite from hydrometallurgical slag). The spent graphite was sieved using stainless steel (400 mesh) to remove impurities such as plastic and metal pieces. Subsequently, after being cleaned with deionized water, the sample was vacuum-dried for 12 hours at 100°C.

Three types of spent graphite were mixed in specific ratios: all graphite from scrap was labeled as sample SG, all graphite from disassembled anodes as sample DG, and all graphite from hydrometallurgical slag as sample HG. A mixture of these graphite in a 1:1:1 ratio. The mixed spent graphite was placed in a quartz tube reaction chamber. The treatment process consisted of two stages. In the first stage, a light electrical flash served as a pretreatment, where the samples, placed in a vacuum tube, were subjected to a 10A electric current after charging several parallel capacitors to 36V. In the second stage, a pulse was applied, releasing a large electric current within a few milliseconds (5ms) after charging several parallel capacitors to 180V. During this process, a “spark” phenomenon was observed. The final product was naturally cooled to room temperature and labeled as sample FG, which was collected as new graphite for lithium-ion batteries (LIBs).

2.2. Characterization of Material

Surface morphology was examined using scanning electron microscopy (SEM, JSM-7610F, JEOL) and transmission electron microscopy (TEM, JEOL 2011). The metal element content was quantified with inductively coupled plasma atomic emission spectrometry (ICP-OES, iCAP 6300, Thermo Scientific). Fourier-transform infrared spectroscopy (FTIR) spectra of this graphite were recorded through a Nexus 670 FTIR spectrometer. Specific surface area and pore size distribution were assessed through Brunauer–Emmett–Teller (BET) and Barrett–Joyner–Halenda (BJH) models using a Micro TriStar II Plus 2.02 analyzer. X-ray diffraction (XRD) with a Bruker D8 was used to investigate the crystal structure of spanning a 5–90° range. Raman spectroscopy was utilized to analyze defects in F-RG and spent graphite performed with a Horiba Jobin-Yvon LabRAM HR800c. Surface characterization was carried out using X-ray photoelectron spectroscopy (XPS) with a Thermo Fisher Escalab Xi+ (Al Kα).

2.3 Electrochemical measurements

The slurry was prepared from graphite, Super-P, and polyvinylidene fluoride (PVDF) in a weight ratio of 8:1:1 and mixed under magnetic stirring until a homogeneous distribution was achieved. It was then coated onto copper foil to a thickness of 300 μm, vacuum-dried at 120°C, and subsequently cut to the required dimensions. Lithium metal served as the reference electrode, with the two electrodes separated by a Celgard 2400 membrane. The electrolyte used was a 1 M LiPF6 solution mixed in a volumetric ratio of 1:1:1 of ethylene carbonate (EC) and dimethyl carbonate (DMC). CR2032 coin-type half-cells were assembled in an argon-filled glove box.

To assess the Electrochemical performance of the batteries, galvanostatic charge/discharge tests were conducted over a voltage span of 0.01 to 3.0 V using a multichannel battery testing system (CT2001A, China). Cyclic Voltammetry (CV) measurements were performed with an electrochemical workstation (CHI 760E, China), scanning from 0.5 mV/s to 2.0 V within the designated potential range. Electrochemical Impedance Spectroscopy (EIS) was executed at open circuit potential, covering a frequency range from 100 kHz to 0.01 Hz.

2.4 Computational method

For all computations in this study, we employed the density functional theory (DFT) method B3LYP with the D3(BJ) dispersion correction.[13] The 6-31G(d) basis set was used for geometry optimizations of the atoms.[14] Vibrational frequency analyses, conducted at the same theoretical level, confirmed that the stationary points were local minima, as evidenced by the absence of imaginary frequencies. Single-point energy calculations were performed with the 6-311+G(d,p) basis set to obtain more accurate energy corrections.[15] All theoretical DFT calculations were executed using the Gaussian 16 software suite.

3. Results and Discussion

3.1 Materials Characterization

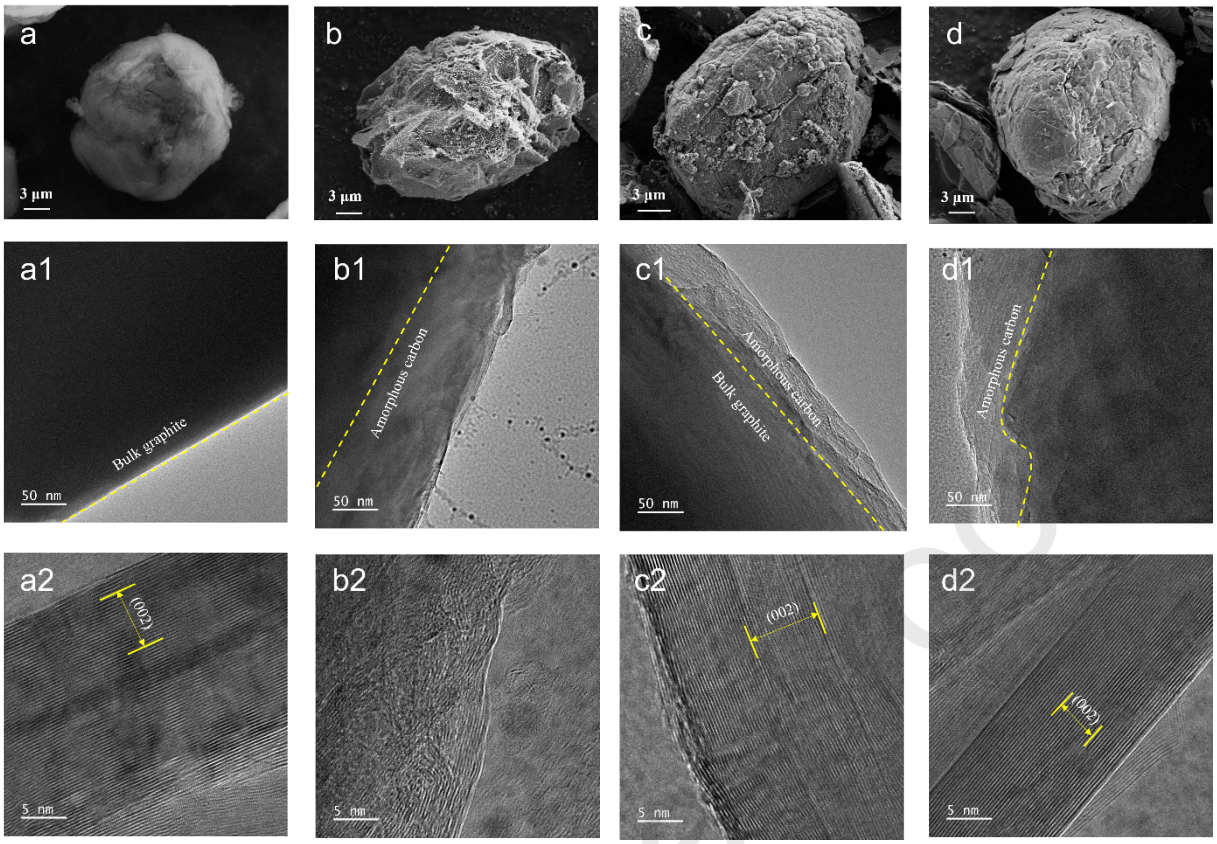

Fig 2. SEM and TEM of various graphite samples at multiple resolutions: (a, a1, a2) flashed mixture graphite (FG); (b, b1,b2) graphite from scrap (SG); (c, c1, c2) graphite from disassembled anode (DG); (d, d1, d2) graphite from hydrometallurgical slag (HG).

Scanning electron microscope (SEM) was used to investigate the morphological characteristics of all the samples. Fig 2a- Fig 2d presents the SEM images of the SG, DG, HG, and FG samples. All samples exhibited spherical structures, indicating that all types of spent graphite are suitable for regeneration into battery-grade material.[9, 16] Unlike FG, which presented a smooth surface, the different spent graphite samples exhibited rough surfaces and significant white substances. As reported in other literature, the structure of graphite from scrap (SG) remains well-preserved despite some impurities coated on, which mainly originate from the employed binder.[16] The well-maintained structure of the graphite from scrap (SG) can be attributed to its lack of participation in the charge and discharge process. Disassembled anode (DG) graphite exhibited various surface imperfections, primarily from conductive agents or binders and participation in the charge and discharge process. Conversely, graphite derived from hydrometallurgical slag (HG) exhibited cracked and partially damaged surface coating layers due to internal stresses within the graphite. This damage allowed Li^+ ions and organic solvents to co-intercalate into the graphite structure. Moreover, the strong acids used in the hydrometallurgical process caused severe degradation of the graphite's surface and structure. In summary, SEM characterization and analysis revealed that HG graphite-layered structure was the most severely compromised, primarily due to high impurity content and significant structural damage. Additionally, the elemental mapping of (HG) graphite derived from hydrometallurgical slag and the (FG) flash-regenerated graphite is presented in Fig S1. Detailed elemental content of various graphite samples is provided in Table S1. These data indicated that the regenerated graphite exhibits an almost complete absence of impurity elements.

For a detailed analysis, TEM characterization was performed on these graphite samples,

demonstrating that an amorphous carbon structure with uneven thickness dominated the surfaces of all spent graphite samples. (Fig 2a1- Fig 2d2). This is ascribed to the organic binders or generated solid electrolyte interface (SEI) during cycling. In contrast, the surface of the flash-regenerated graphite (FG) displayed a distinct bulk graphite layered structure[4, 17]. The image at high-magnification clearly show that interlayer spacing, which consisted with graphite (002) crystal plane. Notably, the interlayer spacing is widened or warped in some samples. The increased interlayer spacing in graphite samples from disassembled anodes is due to the accumulated intermolecular interactions from the repeated embedding and de-embedding of lithium ions during their application period. The warped interlayer spacing observed in graphite from hydrometallurgical slag is attributed to the continuous and harsh separation and purification processes, especially the sulfuric acid treatment in traditional hydrometallurgical methods. [11] While after being repaired by flash Joule heating (FJH) treatment, the image of FG in Fig 2a1 and Fig 2a2 presented bulk graphite without amorphous carbon, and well-aligned interlayers and narrow spacing, which is consistent with XRD and Raman results. These morphological studies suggest that flash recycling process effectively preserves the bulk structure and quality of graphite while preventing the formation of new defects.

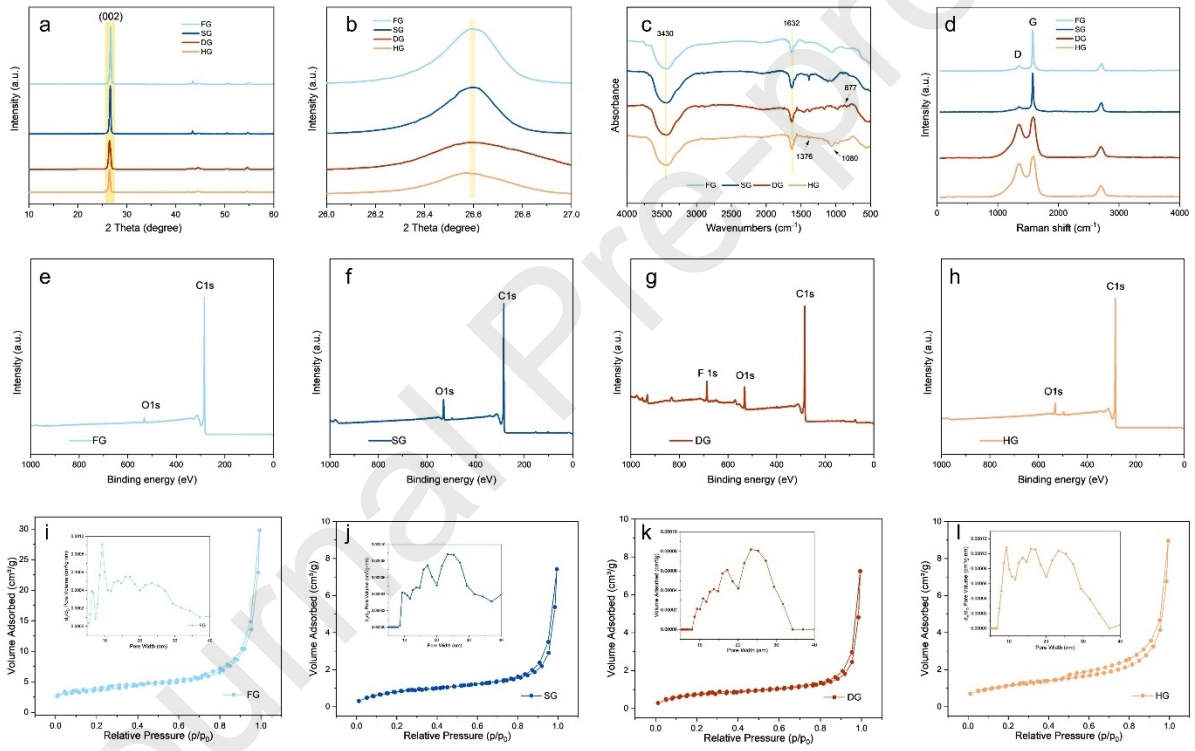

Fig 3. Characterization of various graphite samples: (a) full XRD spectrum; (b) enlargement of XRD spectrum at 2θ = 26-27°; (c) Raman spectroscopy; (d) FTIR spectrum;(e-h) XPS spectra; (i-l) Nitrogen adsorption-desorption isotherms and pore width for various graphite

The physical phases of the spent and regenerated graphite was analyzed using X-ray diffraction (XRD). As illustrated in Fig. 3a and Fig 3b, XRD spectrum for all samples show a strong diffraction peak around 26.6°, according to the (002) crystal plane diffraction of graphite. This peak is consistent with 2H graphite phase, belong to P63/mmc space group (PDF card 41–1487) .[18] Notably, organic contaminants decreases the intensity of the reflection at the (002) plane following rapid high-temperature processing. Fig 3b provides an enlarged view of the (002) peaks, enabling a detailed assessment of differences in interplanar spacing among the samples. The interlayer spacing d (nm) was calculated using Bragg's law: ($2d\sin\theta = n\lambda$, θ is the

diffraction angle, λ(nm) is the wavelength, and n is the reflective series) .[19] An increase in graphite interplanar spacing is indicated by the slight shift in the diffraction peaks observed in the results: the 2θ angle changed from 26.53° of HG, 26.56°of DG 26.59° of SG compared to 26.60° for FG. This phenomenon suggests that a wider interplanar gap between HG and DG caused by insertion and removal of lithium ions in the galvanostatic charge/discharge process. Additionally, a slight shift in the 2θ peak for HG was observed, attributed to extensive acid treatments, which reflect the phenomenon of extra layer expansion.[20] Overall, despite significant damage during the charge-discharge process or hydrometallurgical stage, the flash Joule heating (FJH) method successfully restored all three types of spent graphite into a uniform interlayer spacing of approximately 0.3350 nm, similar to commercial layered graphite structure.[21] This uniform interlayer spacing enhances the immobilization of lithium ions, providing a significant advantage over spent graphite.[22, 23]

To investigate alterations in the functional groups in the materials, FTIR spectroscopy was also performed at 4000-500 cm^{-1} (Fig 3c). Across all samples, an obvious peak corresponding to the -OH stretching vibration was observed at 3430 cm^{-1}, indicating the hygroscopic nature of the graphite samples.[24] The stretching vibrations of the C=C groups within the aromatic ring, which are characteristic of the graphite structure, are represented by prominent and distinct peaks observed at 1632 cm^{-1}.[25] The spectra of graphite from hydrometallurgical slag (HG) and scrap graphite (SG) reveal peaks at 1376 and 1080 cm^{-1}, associated with the presence of polymerized styrene-butadiene rubber (SBR) binder in the spent anode materials.[26] Furthermore, the peaks observed at 877 cm^{-1} in the graphite derived from disassembled anodes (DG) are associated with the presence of CO_3^{2-} in the solid electrolyte interface (SEI). Following the flash Joule heating (FJH) treatment, these peaks diminish or vanish, signifying the elimination of organic molecules.[27]

The effects of flash joule heating (FJH) treatment on graphite regeneration were evaluated using raman spectroscopy at frequencies between 0 and 4000 cm^{-1} (Fig. 3d). The D and G bands were found to be prominently positioned at roughly 1350 and 1570 cm^{-1}, respectively. [19, 28] The G band corresponds to the plane stretching vibration of sp^2 carbon bonds, while the D band is typically associated with structural defects within the carbon structure. The intensity ratio (I_D/I_G) can be ascertained to determine the degree of graphitization.[29] Due to repeated insertion and extraction of lithium ions, the I_D/I_G values for HG and DG are 0.71 and 0.78, respectively, reflecting significant disorder in the carbon structure in the spent graphite. SG processes an I_D/I_G ratio of 0.21, suggesting that the initial graphite structure remains relatively intact.[30] After FJH treatment, the I_D/I_G ratios of various spent graphites converted into 0.18 in FG, indicating that surface carbon disorder has been effectively removed and interlayer defects have been filled and restored, leading to a ordered and uniform graphite structure.

The surface chemical composition of the graphite samples are analyzed with the help of

X-ray photoelectron spectroscopy (XPS). As illustrated in Fig. 3e-Fig. 3h, all samples revealed the presence of carbon (C) and oxygen (O), while a distinct F 1s peak were detected in graphite from the disassembled anode (DG) XPS survey spectrum. The absence of the F 1s peak after flash joule heating (FJH) treatment is owing to the decomposition and volatilization of solid electrolyte interface (SEI), electrolyte, and organic binder. Additionally, the flashed mixture graphite (FG) displayed a pronounced increase in the carbon peak intensity, indicating a significant enrichment of carbon following FJH treatment, the high-resolution C 1s spectra further elucidate the structural changes. For the spent graphite, characteristic peaks are observed at C=C bonds (C=C sp^2, 284.8 eV), C-C bonds (C-C sp^3, 285.1 eV), C-O single bonds (C-O, 285.9 eV), C=O double bonds (C=O, 291.4 eV), and organofluoride groups (CF_2CH_2, 291.66

eV) (Fig. S2).[31] After FJH treatment, the peaks corresponding to carbon-oxygen functional groups and organofluoride components decrease or disappear, while the intensity of the carbon peak in graphite significantly increases. This change is further corroborated by a marked reduction in oxygen content in Table S2, indicating the removal of electrolyte contaminants and residual binder from the surface. Moreover, the C=C sp^2 peak constitutes the predominant carbon species in FG, accounting for 88.44% of the total carbon content, reflecting a higher degree of carbon ordering and a substantial reduction in disordered carbon species. The finding also matches conclusions obtained from XRD and Raman spectroscopy. The O 1s peak analysis reveals two peaks at 532.4 eV and 534.3 eV, the peak shape and peak position of the characteristic peak corresponding to O-C and O=C, respectively.[32] A notable shift in relative proportions was also observed. After FJH treatment, the intensity of the O=C component in DG decreased markedly from 55.79% to that in FG of 33.97%, indicating the decomposition and removal of oxygen-containing functional groups from the SEI, aligning with FTIR analyses. These results indicates that the rapid high-temperature treatment decreases oxygen-related defects and simultaneously improving the ordering of carbon atoms.

Additionally, the nitrogen adsorption-desorption isotherms for all samples are presented in Fig. 3i- Fig. 3l. Specific surface area was derived by the N_2 adsorption data using the multipoint Brunauer-Emmett-Teller (BET) method. The pore width was assessed using the Barrett-Joyner-Halenda (BJH) method. The N_2 adsorption-desorption isotherm curves of the samples exhibit similar profiles, all demonstrating type IV isotherms along with characteristic hysteresis loops.[33] Moreover, the pore sizes of HG are predominantly distributed between 2 and 50 nm, categorizing them as mesoporous materials. In contrast, FG displays a significantly larger surface area of 12.6 m^2/g compared to the spent graphite samples, which include SG (3.27 m^2/g), DG (2.79 m^2/g), and HG (4.84 m^2/g). This increased surface area is owing to the removal of smaller particles and the exfoliation of graphite during the flash joule heating (FJH) process. The enhanced surface area facilitates construct of surface defects, potentially improving the initial coulombic efficiency.[34, 35]

3.2. Electrochemical performance

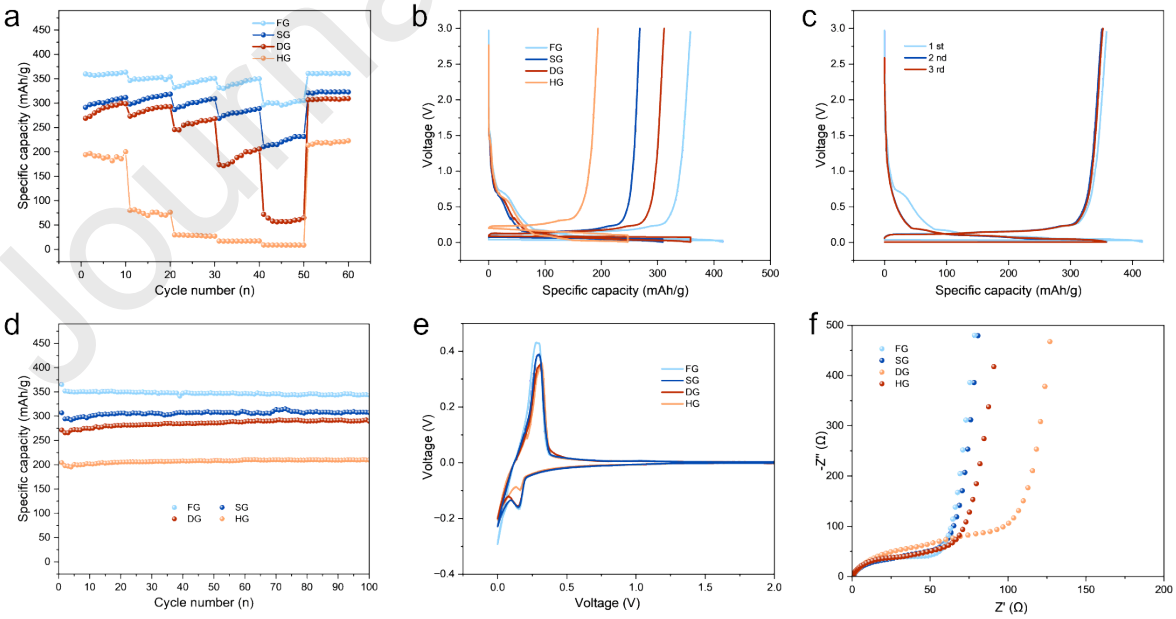

Fig. 4. (a) The rate performance of different materials v at current densities at a current density of 0.1C /0.2C/0.5C/1C/2C/0.1C; (b) First cycle of HG, RG, DG and HG at current

density of 0.1C; (c) first 3 cycles of RG-1000 at the current density of 0.1C; (d) cycle property of HG, RG, DG and HG at the current density of 0.1C; (e) cyclic voltammetry curves of different electrodes;(f) Nyquist plots of different electrodes.

To evaluate the effects of this flash recycling method, the electrochemical properties of different graphite materials were tested using half-cells, focusing on rate performance, initial coulombic efficiency, and electrochemical stability. Rate performance of HG, RG, DG, and FG was tested with a range current densities from 0.1C to 2C are illustrated in Fig. 4a. The charge-specific capacities of FG is 358 mAh/g, 351 mAh/g, 348 mAh/g, 340 mAh/g, and 302 mAh/g at 0.1C, 0.2C, 0.5C, 1C, and 2C current densities. FG demonstrates markedly superior rate performance compared to SG, DG, and HG. In contrast, the HG electrode exhibited the poorest performance, with a 192 mAh/g at 0.1C stable capacity, which decreased significantly to 51 mAh/g at a 2C current density.

Fig. 4b shows the first charge/discharge cycle of the FG electrode, discharge curve depicts a potential plateau with a changing slope as the voltage reduced to about 1.4 V, which implies the solid electrolyte interphase (SEI) film formation. Additionally, a secondary potential plateau emerges as the voltage decreases below 0.4 V, which is associated with the gradual insertion and extraction of solvated lithium ions within the graphite layers. Fig. 4b also demonstrates that the initial coulombic efficiency of FG increases to 87.8%. This improvement is attributed to the removal of surface impurities, which exposes more active sites for lithium-ion interaction and enhances graphite performance [36]. Fig. 4c illustrates that FG maintains improved electrochemical stability after the first cycle, with the structured SEI layer facilitating better lithium-ion transfer [37]. Fig. 4d illustrates the long-term cycling performance of HG, RG, DG, and FG. It showed that after 100 cycles at 0.1C, FG obtains a specific capacity of about 340 mAh/g with a capacity retention of 94.83 %. [38]

To further evaluate and compare the impact of flash heat treatment on its performance, cyclic voltammetry (CV) curves at a scan rate of 0.5 mV/s were conducted on FG, SG, DG, and CG. Fig. 4e presents the CV curves for lithium ion intercalation and deintercalation processes between 0 and 2 V. CV curves for spent and flash-recycled graphite are generally similar, with the oxidation peak of the flash-treated graphite shifting slightly to the left, indicating preserved structural integrity. The reduction peaks and oxidation peaks are at around 0.16 Vand 0.25 V corresponding to the lithiation and deintercalation processes of lithium ion in the graphite intercalation sites, respectively.[18, 39] Among all samples, FG exhibits the highest induced current, highlighting the enhanced electrochemical reactivity of the regenerated graphite. Fig. 4f displays the results of electrochemical impedance spectroscopy (EIS) of all sample. The EIS spectra of the different samples exhibit similar characteristics, featuring semicircle in mid-frequency range and a sloping line in low-frequency range.[40] Typically, semicircle diameter in high-frequency range reflects the charge transfer resistance (R_{CT}), while the slope at low frequencies is closely relationship with the Warburg impedance associated with lithium ion diffusion within the electrode.[41, 42] This findings indicate that the flash-recycled graphite exhibits a lower R_{CT} value compared to all the spent graphite samples. This decrease in charge transfer resistance signifies an improvement in the transport of lithium ions between the phase interfaces, facilitated by the elimination of coating impurities and enhanced interaction between the electrode and electrolyte.

3.3. Economic and Environmental analyses

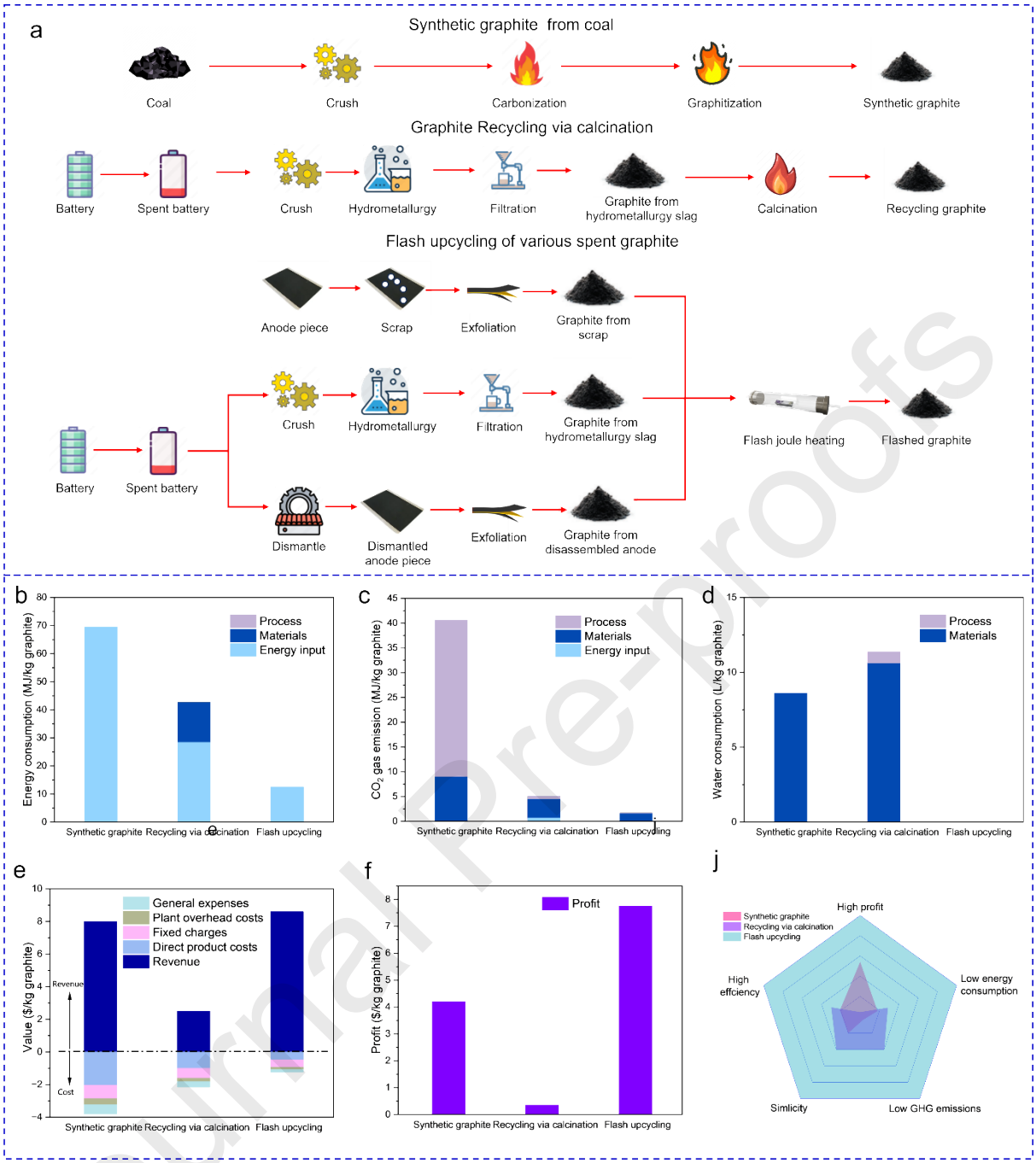

Fig. 5. Economic and environmental analysis: (a) Schematic diagram showing the manufacturing of graphite anodes produced artificial graphite, recycling via calcination and flash upcycling of various graphite; (b) energy consumption; (c) CO_2 emissions; (d) water consumption; (e) value; (f) profit for manufacturing 1 kg graphite and (g) spider chart of these three processes.

The economic and environmental merits of the proposed direct recycling approach were further evaluated by employing the Everbatt 2020 model.[43] Per the schematic delineated in Fig. 5a, the production of artificial graphite and recycling via calcination involve entailing elevated temperature smelting and unnecessary chemical consumption, renowned for their energy-intensive and ecologically injurious attributes. In sharp contrast, our upcycling process not only generated various graphite into uniform properties, but also could take the best advantages of joule heat produced during the flash upcycling process, which could have a direct

effect on the spent graphite.[28] The detailed parameters of total energy consumption, CO_2 emissions, water consumption, and cost of manufacturing 1 kg graphite are delineated in Fig. 5b–f.

In comparison to artificial graphite production, this flash upcycling of various graphite methods could reduce approximately 82.0% energy consumption, and 95.8% CO_2 emissions, slash water usage by 100% and curtail the recycling expenditure by around 67.1%. And comparison to recycling via the calcination process, the decreased energy consumption number was 70.8%, 66.1% CO_2 emissions, and save cost of 41.8%. Furthermore, the profit of produced artificial graphite is 4.2/kg, while the recycling via calcination is nearly zero (0.35), which could be attributed to the rebuilt collapse of the graphite structures and the hydrometallurgy process.[29] Notably, the flash upcycling method of various graphite can achieve a profit of 7.75$/kg, which is significantly higher than the method of producing graphite (4.2$/kg) and recycling via calcination (0.35$/kg). The spider chart of Fig.5g provides a comprehensive comparison of three graphite production and recycling methods—artificial graphite production, traditional calcination recycling, and flash upcycling. These methods are evaluated based on several criteria, including high profitability, low energy consumption, low greenhouse gas (GHG) emissions, simplicity, and high efficiency. Inspiringly, this method behaved a rapid upcycling time and the regenerated graphite exhibited an attractive lithium-storage capability. On the other hand, flash upcycling demonstrates the capability to process a diverse range of graphite materials, offering a simplified procedure and high efficiency. To a clear understanding, the comparson of these recycling method are presented in Table 1. The calculated profit also supports its economic viability. Collectively, these results suggest that the proposed flash upcycling method holds substantial potential for large-scale industrial application in the recovery of various spent graphite anodes.

372 **Table 1. The feature of regenerated graphite using different repair methods**

Raw materials	Method	Temperature	Cycling time	Rate performance	Ref
Mixed spent graphite	Flash joule heating	3000°C	＜1s	358 mAh/g at 0.1C	This work
Black powder	H_2SO_4 curing-anaerobic calcination	1500 °C	2 h	349 mAh/g at 0.1 C	[19]
Black powder	H_2SO_4 leaching-NaOH fusion	500 °C	NaOH fusion 40 min	377.3 mAh/g at 0.1 C	[44]
Black powder	H_2SO_4 leaching-calcination-pitch coating	3000 °C	leaching 4h + coating 2h	344 mAh/g at 0.2C	[45]
Black powder	Roasting	1600 °C	1h	235.0 mAh/g at 1 C	[46]
Black powder	Synthesis of nano-Sn/G@C	1000 °C	2 h	650.9 mAh/g at 100 mA/g	[47]
Black powder	H_2SO_4 leaching-pitch coating	1100 °C	2h	338.2 mAh/g at 0.1C	[20]
Black powder	Carbon coating	800 °C	1h	384.9 mAh/g after 100 cycles	[48]
Disassembled anode	H_2SO_4 leaching-heat-	900 °C	2h	358.1 mAh/g at 0.1C	[31]
Disassembled anode	Anaerobic calcination	1340°C	4h	360.8 mAh/g at 1C	[49]
Disassembled anode	Microwave-irradiation	/	15 s	400 mAh/g at 0.1 Ah/g	[50]

Scrap	Calcination	800°C	2h	362.4 mAh/g at 0.1C	[51]

373

374

375

376

377 **3.4. Analysis of various spent graphite regeneration mechanism**

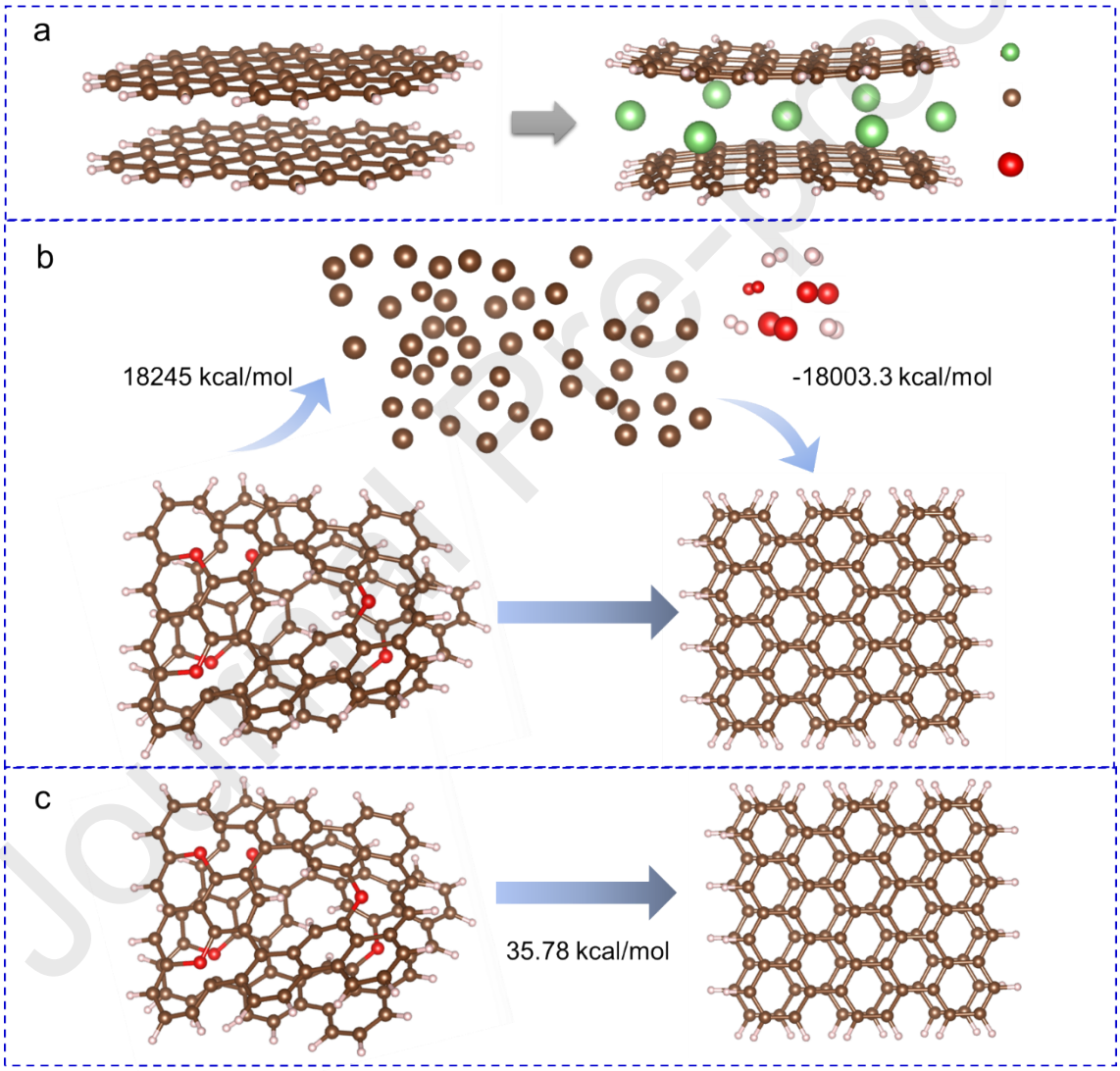

378

379 **Fig. 6. The mechanism of graphite regeneration by flash joule heating treatment:(a)**
380 **Simulation results of graphite intercalation layer degradation,(b) the reconstruction of**
381 **spent graphite structure by traditional calcination process (c) reconstruction of spent**
382 **graphite structure by flash upcycling process.**

Fig.6 illustrates the mechanism of graphite regeneration through flash Joule heating treatment. As shown in Fig. 6a, the graphite layers undergo expansion or deformation due to the insertion and removal of lithium ions, which indicates that lithium ions can easily intercalate into the graphite layers, leading to structural deformation. Fig. 6b shows that graphitizing spent graphite into a stable, ordered layered structure requires an energy of 241.7 kcal/mol. The primary process can be clarified as follows: this suggests that the transformation of a defective graphite structure, with defects introduced by oxygen, occurs as carbon atoms, initially isolated with high freedom, gradually align themselves. Eventually, these randomly distributed carbon atoms in the spent graphite form a stable graphite structure. This result also supports the thermodynamic feasibility of using traditional calcination processes for graphite recycling, although these processes require several hours to achieve optimal repair results.[19] Fig. 6c illustrates the reconstruction of the spent graphite structure through flash upcycling processes. Unlike the traditional calcination process, the flash upcycling process protects carbon atoms from being isolated. As an electric current passes through the carbon atoms, a high current density and a consequently high localized electric field are generated on the surface of the carbon atoms. This electric current energetically favors the reorientation of the graphene layers along the direction of the electric field and the ordering of the graphitic lattice, reducing interlayer spacing. [44] Remarkably, this process consumes much less energy, requiring only 35.8 kcal/mol (based on the energy input needed to generate 1 kg of graphite) .[45]

In summary, our method significantly accelerates the reaction rate, regenerating graphite within seconds. The current in flash Joule heating follows the path of least resistance, rapidly concentrating heat. This intense and localized heating creates optimal thermal conditions for graphite.[28] Consequently, under extreme temperatures and efficient heat utilization, defects caused by oxygen are replaced by free carbon atoms, facilitating the rapid conversion of a disordered structure into an ordered layered structure.

4. Conclusions

In summary, we have proposed an ultrafast and cost-effective method for upcycling various spent graphite materials using flash Joule heating. This method achieves a 358 mAh/g specific capacity and exhibits outstanding cycle stability. Characterization and electrochemical performance analyses reveal that the method effectively removes coated impurities, realigns warped or enlarged graphite layers, and fills defects within the carbon network surface. Environmental and economic impact assessments by the EverBatt model highlight that this method consumes the least energy and material, generates the lowest greenhouse gas emissions, and offers the highest profitability compared to traditional hydrometallurgical recycling processes. Consequently, this study presents a viable technical process for the direct recycling of diverse spent graphite materials, with substantial potential for large-scale industrial implementation.

Conflict of Interests

The authors declare no conflict of interests.

References

[1] G. Harper, R. Sommerville, E. Kendrick, L. Driscoll, P. Slater, R. Stolkin, A. Walton, P. Christensen, O. Heidrich, S. Lambert, A. Abbott, K. Ryder, L. Gaines, P. Anderson, Recycling lithium-ion batteries from electric vehicles, Nature 575(7781) (2019) 75-86. https://doi.org/10.1038/s41586-019-1682-5.

[2] D. Castelvecchi, Electric cars and batteries: how will the world produce enough?, Nature 596 (2021) 336-339. https://doi.org/10.1038/d41586-019-03424-2.

[3] Z. Dong, H. Hao, X. Sun, D. Xun, H. Dou, J. Geng, M. Liu, Y. Deng, F. Zhao, Z. Liu, Projecting future critical material demand and recycling from China's electric passenger vehicles considering vehicle segment heterogeneity, Resources, Conservation and Recycling 207 (2024) 107691-107702. https://doi.org/10.1016/j.resconrec.2024.107691.

[4] K. Jia, G. Yang, Y. He, Z. Cao, J. Gao, H. Zhao, Z. Piao, J. Wang, A.M. Abdelkader, Z. Liang, R.V. Kumar, G. Zhou, S. Ding, K. Xi, Degradation Mechanisms of Electrodes Promotes Direct Regeneration of Spent Li - Ion Batteries: A Review, Adv. Mater. 36(23) (2024). https://doi.org/10.1002/adma.202313273.

[5] J.J. Roy, D.M. Phuong, V. Verma, R. Chaudhary, M. Carboni, D. Meyer, B. Cao, M. Srinivasan, Direct recycling of Li-ion batteries from cell to pack level: Challenges and prospects on technology, scalability, sustainability, and economics, Carbon Energy (2024) e492. https://doi.org/10.1002/cey2.492.

[6] B. Niu, J. Xiao, Z. Xu, Advances and challenges in anode graphite recycling from spent lithium-ion batteries, J. Hazard. Mater. 439 (2022) 129678-129699. https://doi.org/10.1016/j.jhazmat.2022.129678.

[7] J. Liu, H. Shi, X. Hu, Y. Geng, L. Yang, P. Shao, X. Luo, Critical strategies for recycling process of graphite from spent lithium-ion batteries: A review, Sci. Total Environ. 816 (2022) 151621-151623. https://doi.org/10.1016/j.scitotenv.2021.151621.

[8] S. Natarajan, M.L. Divya, V. Aravindan, Should we recycle the graphite from spent lithium-ion batteries? The untold story of graphite with the importance of recycling, Journal of Energy Chemistry 71 (2022) 351-369. https://doi.org/10.1016/j.jechem.2022.04.012.

[9] Z. Shang, W. Yu, J. Zhou, X. Zhou, Z. Zeng, R. Tursun, X. Liu, S. Xu, Recycling of spent lithium-ion batteries in view of graphite recovery: A review, eTransportation 20 (2024) 100320-100348. https://doi.org/10.1016/j.etran.2024.100320.

[10] X. Meng, Y. Xu, H. Cao, X. Lin, P. Ning, Y. Zhang, Y.G. Garcia, Z. Sun, Internal failure of anode materials for lithium batteries — A critical review, Green Energy & Environment 5(1) (2020) 22-36. https://doi.org/10.1016/j.gee.2019.10.003.

[11] Y. Guo, F. Li, H. Zhu, G. Li, J. Huang, W. He, Leaching lithium from the anode electrode materials of spent lithium-ion batteries by hydrochloric acid (HCl), Waste Management 51 (2016) 227-233. https://doi.org/10.1016/j.wasman.2015.11.036.

[12] S. Dühnen, J. Betz, M. Kolek, R. Schmuch, M. Winter, T. Placke, Toward Green Battery Cells: Perspective on Materials and Technologies, Small Methods 4(7) (2020) 2000039. https://doi.org/10.1002/smtd.202000039.

[13] C.R.C. Rêgo, L.N. Oliveira, P. Tereshchuk, J.L.F. Da Silva, Comparative study of van der Waals corrections to the bulk properties of graphite, J. Phys.: Condens. Matter 27(41) (2015) 415502. https://doi.org/10.1088/0953-8984/27/41/415502.

[14] Y. Song, Theoretical study on the electrochemical behavior of norepinephrine at Nafion multi-walled carbon nanotubes modified pyrolytic graphite electrode, Spectrochimica Acta Part A: Molecular and Biomolecular Spectroscopy 67(5) (2007) 1169-1177. https://doi.org/10.1016/j.saa.2006.10.004.

[15] F. Hasager, O.J. Nielsen, K.V. Mikkelsen, Geometries, molecular Rayleigh scattering, Raman and infrared frequencies of polycyclic aromatic hydrocarbons and subunits of graphite studied by DFT methods, Environmental Science: Atmospheres 2(5) (2022) 1023-1031. https://doi.org/10.1039/d1ea00105a.

[16] M. Olutogun, A. Vanderbruggen, C. Frey, M. Rudolph, D. Bresser, S. Passerini, Recycled graphite for more sustainable lithium - ion batteries, Carbon Energy (2024) 483. https://doi.org/10.1002/cey2.483.

[17] T. Li, L. Tao, L. Xu, T. Meng, B.C. Clifford, S. Li, X. Zhao, J. Rao, F. Lin, L. Hu, Direct and Rapid High - Temperature Upcycling of Degraded Graphite, Adv. Funct. Mater. 33(43) (2023). https://doi.org/10.1002/adfm.202302951.

[18] Q. Chen, L. Huang, J. Liu, Y. Luo, Y. Chen, A new approach to regenerate high-performance graphite from spent lithium-ion batteries, Carbon 189 (2022) 293-304. https://doi.org/10.1016/j.carbon.2021.12.072.

[19] Y. Gao, C. Wang, J. Zhang, Q. Jing, B. Ma, Y. Chen, W. Zhang, Graphite Recycling from the Spent Lithium-Ion Batteries by Sulfuric Acid Curing–Leaching Combined with High-Temperature Calcination, ACS Sustainable Chemistry & Engineering 8(25) (2020) 9447-9455. https://doi.org/10.1021/acssuschemeng.0c02321.

[20] H. Da, M. Gan, D. Jiang, C. Xing, Z. Zhang, L. Fei, Y. Cai, H. Zhang, S. Zhang, Epitaxial Regeneration of Spent Graphite Anode Material by an Eco-friendly In-Depth Purification Route, ACS Sustainable Chemistry & Engineering 9(48) (2021) 16192-16202. https://doi.org/10.1021/acssuschemeng.1c05374.

[21] G.Q. Yu, M.-Z. Xie, Z.-H. Zheng, Z.-G. Wu, H.-L. Zhao, F.-Q. Liu, Efficiently regenerating spent lithium battery graphite anode materials through heat treatment processes for impurity dissipation and crystal structure repair, Resources, Conservation and Recycling 199 (2023) 107267-107275. https://doi.org/10.1016/j.resconrec.2023.107267.

[22] H.J. Liang, B.-H. Hou, W.-H. Li, Q.-L. Ning, X. Yang, Z.-Y. Gu, X.-J. Nie, G. Wang, X.-L. Wu, Staging Na/K-ion de-/intercalation of graphite retrieved from spent Li-ion batteries: in operando X-ray diffraction studies and an advanced anode material for Na/K-ion batteries, Energy & Environmental Science 12(12) (2019) 3575-3584. https://doi.org/10.1039/c9ee02759a.

[23] S. Natarajan, V. Aravindan, An Urgent Call to Spent LIB Recycling: Whys and Wherefores for Graphite Recovery, Advanced Energy Materials 10(37) (2020) 2002238-2002246. https://doi.org/10.1002/aenm.202002238.

[24] Y. Lai, X. Zhu, J. Li, Q. Gou, M. Li, A. Xia, Y. Huang, X. Zhu, Q. Liao, Recovery and regeneration of anode graphite from spent lithium-ion batteries through deep eutectic solvent treatment: Structural characteristics, electrochemical performance and regeneration mechanism, Chem. Eng. J. 457 (2023) 141196-141203. https://doi.org/10.1016/j.cej.2022.141196.

[25] S. Dong, Y. Song, K. Ye, J. Yan, G. Wang, K. Zhu, D. Cao, Ultra-fast, low-cost, and green regeneration of graphite anode using flash joule heating method, EcoMat 4(5) (2022). https://doi.org/10.1002/eom2.12212.

[26] Q. Lu, M. Wang, Z. Peng, Innovative Method to Recover Graphite from Spent Lithium-Ion Batteries, ACS Sustainable Chemistry & Engineering 12(16) (2024) 6157-6168. https://doi.org/10.1021/acssuschemeng.3c07744.

[27] V. Ţucureanu, A. Matei, A.M. Avram, FTIR Spectroscopy for Carbon Family Study, Crit. Rev. Anal. Chem. 46(6) (2016) 502-520. https://doi.org/10.1080/10408347.2016.1157013.

[28] D.X. Luong, K.V. Bets, W.A. Algozeeb, M.G. Stanford, C. Kittrell, W. Chen, R.V. Salvatierra, M. Ren, E.A. McHugh, P.A. Advincula, Z. Wang, M. Bhatt, H. Guo, V. Mancevski, R. Shahsavari, B.I. Yakobson, J.M. Tour, Gram-scale bottom-up flash graphene synthesis, Nature 577(7792) (2020) 647-651. https://doi.org/10.1038/s41586-020-1938-0.

[29] Y. Li, W. Lv, H. Zhao, Y. Xie, D. Ruan, Z. Sun, Regeneration of anode materials from complex graphite residue in spent lithium-ion battery recycling process, Green Chem. 24(23) (2022) 9315-9328. https://doi.org/10.1039/d2gc02439j.

[30] H. Yu, H. Dai, Y. Zhu, H. Hu, R. Zhao, B. Wu, D. Chen, Mechanistic insights into the lattice reconfiguration of the anode graphite recycled from spent high-power lithium-ion batteries, J. Power Sources 481 (2021) 229159-229172. https://doi.org/10.1016/j.jpowsour.2020.229159.

[31] Y. Gao, J. Zhang, H. Jin, G. Liang, L. Ma, Y. Chen, C. Wang, Regenerating spent graphite from scrapped lithium-ion battery by high-temperature treatment, Carbon 189 (2022) 493-502. https://doi.org/10.1016/j.carbon.2021.12.053.

[32] M. Gu, L. Fan, J. Zhou, A.M. Rao, B. Lu, Regulating Solvent Molecule Coordination with KPF6 for Superstable Graphite Potassium Anodes, ACS Nano 15(5) (2021) 9167-9175. https://doi.org/10.1021/acsnano.1c02727.

[33] Z. Shang, X. An, H. Zhang, M. Shen, F. Baker, Y. Liu, L. Liu, J. Yang, H. Cao, Q. Xu, H. Liu, Y. Ni, Houttuynia-derived nitrogen-doped hierarchically porous carbon for high-performance supercapacitor, Carbon 161 (2020) 62-70. https://doi.org/10.1016/j.carbon.2020.01.020.

[34] Y. Yang, S. Song, S. Lei, W. Sun, H. Hou, F. Jiang, X. Ji, W. Zhao, Y. Hu, A process for combination of recycling lithium and regenerating graphite from spent lithium-ion battery, Waste Management 85 (2019) 529-537. https://doi.org/10.1016/j.wasman.2019.01.008.

[35] H. Wang, Y. Huang, C. Huang, X. Wang, K. Wang, H. Chen, S. Liu, Y. Wu, K. Xu, W. Li, Reclaiming graphite from spent lithium ion batteries ecologically and economically, Electrochim. Acta 313 (2019) 423-431. https://doi.org/10.1016/j.electacta.2019.05.050.

[36] H. Zhang, Y. Yang, D. Ren, L. Wang, X. He, Graphite as anode materials: Fundamental mechanism, recent progress and advances, Energy Storage Materials 36 (2021) 147-170. https://doi.org/10.1016/j.ensm.2020.12.027.

[37] H. Da, S. Pan, J. Li, J. Huang, X. Yuan, H. Dong, J. Liu, H. Zhang, Greatly recovered electrochemical performances of regenerated graphite anode enabled by an artificial PMMA solid electrolyte interphase layer, Energy Storage Materials 56 (2023) 457-467. https://doi.org/10.1016/j.ensm.2023.01.038.

[38] K. Chen, Y. Ding, L. Yang, Z. Wang, H. Yu, D. Fang, Y. Feng, L. Hu, C. Xu, P. Shao, X. Luo, L. Chen, Recycling of spent lithium–ion battery graphite anodes via a targeted repair scheme, Resources, Conservation and Recycling 201 (2024) 107326-107336. https://doi.org/10.1016/j.resconrec.2023.107326.

[39] J. Yang, E. Fan, J. Lin, F. Arshad, X. Zhang, H. Wang, F. Wu, R. Chen, L. Li, Recovery and Reuse of Anode Graphite from Spent Lithium-Ion Batteries via Citric Acid Leaching, ACS Applied Energy Materials 4(6) (2021) 6261-6268. https://doi.org/10.1021/acsaem.1c01029.

[40] F. Lai, X. Zhang, Q. Wu, J. Zhang, Q. Li, Y. Huang, Z. Liao, H. Wang, Effect of Surface Modification with Spinel NiFe2O4 on Enhanced Cyclic Stability of LiMn2O4 Cathode Material in Lithium Ion Batteries, ACS Sustainable Chemistry & Engineering 6(1) (2017) 570-578. https://doi.org/10.1021/acssuschemeng.7b02876.

[41] S. Tu, Z. Lu, M. Zheng, Z. Chen, X. Wang, Z. Cai, C. Chen, L. Wang, C. Li, Z.W. Seh, S. Zhang, J. Lu, Y. Sun, Single - Layer - Particle Electrode Design for Practical Fast - Charging Lithium - Ion Batteries, Adv. Mater. (Weinheim, Ger.) 34(39) (2022) 2202892. https://doi.org/10.1002/adma.202202892.

[42] W.E. Gent, G.M. Busse, K.Z. House, The predicted persistence of cobalt in lithium-ion batteries, Nature Energy 7(12) (2022) 1132-1143. https://doi.org/10.1038/s41560-022-01129-z.

[43] Q. Dai, J. Spangenberger, S. Ahmed, L. Gaines, J.C. Kelly, M. Wang, EverBatt: A Closed-loop Battery Recycling Cost and Environmental Impacts Model, United States, 2019, p. Medium: ED; Size: 88 p.

[44] L. Eddy, S. Xu, C. Liu, P. Scotland, W. Chen, J.L. Beckham, B. Damasceno, C.H. Choi, K. Silva, A. Lathem, Y. Han, B.I. Yakobson, X. Zhang, Y. Zhao, J.M. Tour, Electric Field Effects in Flash Joule Heating Synthesis, J. Am. Chem. Soc. 146(23) (2024) 16010-16019. https://doi.org/10.1021/jacs.4c02864.

[45] W. Chen, R.V. Salvatierra, J.T. Li, C. Kittrell, J.L. Beckham, K.M. Wyss, N. La, P.E. Savas, C. Ge, P.A. Advincula, P. Scotland, L. Eddy, B. Deng, Z. Yuan, J.M. Tour, Flash Recycling of Graphite Anodes, Adv. Mater. (Weinheim, Ger.) 35(8) (2022) 2207303. https://doi.org/10.1002/adma.202207303.

Highlights:

- Different types of spent graphite can be regenerated into uniform, battery-grade graphite material within seconds.

- This recycling method can significantly increase profitability, reduce total energy consumption with a less greenhouse gas emission
- The mechanism of flash joule heating transforms various spent graphite into uniformity property are revealed and verified.
- Density Functional Theory (DFT) calculations confirm that flash joule heating enables direct regeneration at a high reaction rate

Declaration of interests

☒ The authors declare that they have no known competing financial interests or personal relationships that could have appeared to influence the work reported in this paper.

☐ The authors declare the following financial interests/personal relationships which may be considered as potential competing interests:

Conflict statement: